

Chapter 10

Ultra-discretization of Nonlinear Control Systems with Spatial Symmetry

Masato Ishikawa and Takuto Kita

10.1 Introduction

Nonlinear control systems, as well as nonlinear dynamical systems in general, are usually referred to nonlinear ordinary differential equations expressed by $\dot{x} = f(x, u)$, where $x \in M$ is its state, M is a smooth manifold of states, $u \in U \subset \mathbb{R}^m$ is the control input included in the set of admissible controls U , and f if a smooth mapping $f : M \times U \rightarrow TM$.

Now, let us think of its *discrete alternative in full sense*, i.e., behavior of a system whose variables are all discrete with respect to *spacio-temporal* axes. Suppose M_d is a finite set corresponding to a discrete version of the state space, U_d is also a finite set of admissible control symbols. Then consider a discrete-valued *difference* equation

$$x[k + 1] = f_d(x[k], u[k]), \quad x \in M_d, u \in U_d, f_d : M_d \times U_d \rightarrow M_d$$

where $k \in \mathbb{Z}$ denotes the time step instead of the continuous time $t \in \mathbb{R}$. This approach is often called *em ultra-discretization*, mainly along the context of mathematical analysis of integrable systems such as various soliton equations [3]. The prefix *ultra*-distinguishes the problem from so-called discrete-time systems, in the sense that the dependent variable x is supposed discrete, as well as the independent variable k . Upon facing to these ultra-discrete control systems, we are naturally led to discuss which sort of controller *design* framework (i.e., how to design a state

M. Ishikawa (✉) · T. Kita
Department of Mechanical Engineering, Osaka University,
2-1 Yamadaoka, Suita, Osaka 565-0871, Japan
e-mail: ishikawa@mech.eng.osaka-u.ac.jp

T. Kita
Denso Co. Ltd., Kosai, Japan

feedback law $u[k] = k(x[k])$ to fulfill the design requirement) can be established. This is the central motivation in this chapter.

It would be technically possible to develop systems theory for *general* class of M_d , U_d and f_d . However, in this chapter, we dare to confine ourselves to a specific class of systems in the following manners:

- M_d is not only a mere collection of elements, but is associated with some structure such as *symmetry*.
- There exist some *first principles* behind the system dynamics. In other words, f_d should be derived from some discrete version of first principles, not by straightforward discretization of f (see Fig. 10.4 below).

From these points of view, in this chapter, we consider to discuss discrete-valued alternative of *planar locomotion* of rigid bodies. Planar locomotion is inherently symmetric under isometric transformation, i.e., invariant under action of translation and rotation without mirror reflection. The set of such a transformation is identified with the special Euclidean transformation group, say $\mathbb{SE}(2)$, parameterized by $\{(x, y, \theta) | x \in \mathbb{R}, y \in \mathbb{R}, \theta \in \mathbb{S}\} \simeq \mathbb{R}^2 \times \mathbb{S}$. The configuration space of the vehicle $\mathbb{SE}(2)$ is supposed to be discretized as a hexagonal cellular space [6], while the shape space (or joint space, usually referred to \mathbb{T}^n) is also discretized as \mathbb{Z}_6^n of modular arithmetic.

Control problems in planar locomotion have been attracting much interest of nonlinear control theorists and robotics researchers since early 90s. Some notable properties of such a system include: (1) the set of equilibria forms a submanifold of the state space rather than an isolated point, (2) any equilibrium cannot be asymptotically stabilized by continuous state feedback as pointed out by Brockett [2], (3) nevertheless the equilibrium can be reached from its neighborhood if it satisfies the Lie algebra rank condition [10]. As the conventional control theory of planar locomotion is based on nonintegrable nature of kinematic constraints, we start from considering a discrete-valued version of nonholonomic constraints (an integer-valued equation of integer variables), then discuss how the admissible motion that satisfies the constraint look, compared to the continuous ones. Here we re-emphasize that the issue addressed here is (relevant, though) different from a *discretization* of continuous nonlinear systems or nonlinear *sampled-data* systems [1, 7, 9, 13]. In other words, the resulting behavior can rather be viewed as a special class of *cellular automata* [11, 12]. Our standpoint is just to observe what should happen, starting from the discrete constraints as principal rules. This chapter partially includes the results obtained by the authors, reported in [4].

In the rest of the chapter, $t \in \mathbb{R}$ denotes the time in continuous case, while $k \in \mathbb{Z}$ denotes the time *step* in discrete case. Moreover, we often use the following short-form notation, $C_i := \cos \theta_i$, $S_i := \sin \theta_i$, $C_{ij} := \cos(\theta_i - \theta_j)$ and $S_{ij} := \sin(\theta_i - \theta_j)$ to save the space.

10.2 Basic Properties on the Hexagonal Cellular Space

10.2.1 Coordinate Settings

Suppose a tessellation of two-dimensional euclidean space \mathbb{R}^2 with *unit hexagons*, as shown in Fig. 10.1. Let O be a center of a hexagon. The x -axis is the line passing through O which is assumed perpendicular to the edge of a hexagon, while y -axis passes through one of its vertex (alternative definition can be possible). Here we introduce the following three constants will play important roles throughout this chapter,

$$\alpha = \frac{1}{2}, \beta = \frac{\sqrt{3}}{2}, \gamma = \frac{\pi}{3},$$

which satisfy following elementary relations

$$\alpha^2 + \beta^2 = 1, \alpha^2 - \beta^2 = -\alpha.$$

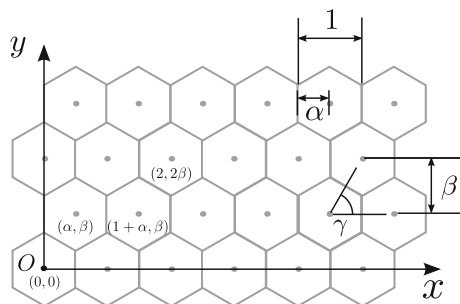
Each cell is identified with the (x, y) -position of its center, e.g., (α, β) , $(1 + \alpha, \beta)$ or $(2, 2\beta)$ in Fig. 10.1.

For θ refers to an angle on this space, it should be confined to $0, \pm\gamma, \pm2\gamma, \pm3\gamma, \dots$, where 3γ and -3γ are identified to each other. As slight abuse of notation, we identify γi ($i \in \mathbb{Z}$) with i itself, as long as it causes no confusion. In other words, the space of angles is identified with the set of integers modulo 6:

$$\mathbb{Z}_6 = \{0, 1, 2, 3, 4, 5\} \equiv \{0, \pm 1, \pm 2, 3\},$$

The integer $3 \in \mathbb{Z}_6$ will be treated as discrete counterpart of $\pi \in \mathbb{S}$. Similarly, $\cos \theta$ actually implies $\cos \gamma\theta$ for any discrete angle $\theta \in \mathbb{Z}_6$. The cosine and sine of discrete angles are summarized in Fig. 10.2. Fundamental trigonometric identities, such as angle addition formulae, naturally hold as in the continuous case.

Fig. 10.1 Coordinate settings on the hexagonal cellular space and the unitary constants used for the coordinates



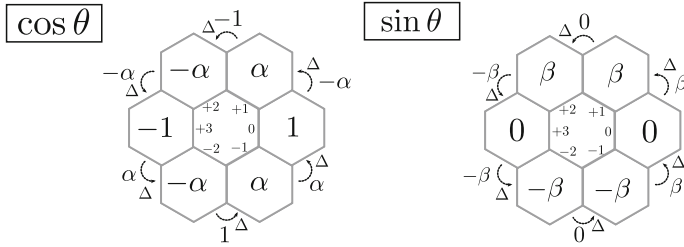


Fig. 10.2 Cosine (*left*) and sine (*right*) functions defined on the hexagonal cells. The symbols shown in the cells indicate values of functions at corresponding direction (e.g., $\cos(1) = \alpha$). Symbols shown between two cells indicate their differences (e.g., $\cos(2) - \cos(1) = (-\alpha) - \alpha = -1$.)

In summary, we define the whole configuration space of planar rigid body, say $\mathbb{S}\mathbb{E}_H(2)$, as follows:

$$\mathbb{S}\mathbb{E}_d(2) = \left\{ \begin{bmatrix} x \\ y \\ \theta \end{bmatrix} = \begin{bmatrix} n_x + \text{odd}(y)\alpha \\ n_y\beta \\ n_\theta \end{bmatrix} \middle| n_x, n_y \in \mathbb{Z}, n_\theta \in \mathbb{Z}_6 \right\} \simeq \mathbb{Z} \times \mathbb{Z} \times \mathbb{Z}_6, \tag{10.1}$$

where $\text{odd}(y)$ is 1 if y is an odd integer, 0 otherwise.

10.2.2 Basics of Difference Calculus in Concern

For a function $f(\theta)$, we define

$$\Delta_\theta f := f(\theta + \Delta\theta) - f(\theta),$$

where $|\Delta\theta| \leq 1$. $\Delta_\theta f$ is simply denoted by Δf if the argument is obvious. Note that Δf depends on both θ and $\Delta\theta$. By definition, $\Delta f = 0$ if $\Delta\theta = 0$.

Differentiation of trigonometric functions are derived as follows. First, note that cosine and sine of small angles are formulated by (see Fig. 10.2)

$$\cos \Delta\theta = 1 - \alpha\Delta\theta^2, \quad \sin \Delta\theta = \beta\Delta\theta \quad (\text{if } |\Delta\theta| \leq 1).$$

Therefore

$$\begin{aligned} \cos(\theta + \Delta\theta) - \cos \theta &= \cos \theta \cos \Delta\theta - \sin \theta \sin \Delta\theta - \cos \theta \\ &= -\sin \Delta\theta \sin \theta + (\cos \Delta\theta - 1) \cos \theta \\ &= -\beta\Delta\theta \sin \theta - \alpha\Delta\theta^2 \cos \theta, \end{aligned}$$

Table 10.1 Discrete version of calculus; differences of trigonometric functions for $|\Delta\theta| = 1$

$\Delta \cos \theta$						
	$\theta = -2$	$\theta = -1$	$\theta = 0$	$\theta = 1$	$\theta = 2$	$\theta = 3$
$\Delta\theta = 1$ (i.e., $\cos(\theta + 1) - \cos\theta$)	1	α	$-\alpha$	-1	$-\alpha$	α
$\Delta\theta = -1$ (i.e., $\cos(\theta - 1) - \cos\theta$)	$-\alpha$	-1	$-\alpha$	α	1	α
$\Delta \sin \theta$						
$\Delta\theta = 1$ (i.e., $\sin(\theta + 1) - \sin\theta$)	0	β	β	0	$-\beta$	$-\beta$
$\Delta\theta = -1$ (i.e., $\sin(\theta - 1) - \sin\theta$)	β	0	$-\beta$	$-\beta$	0	β

$$\begin{aligned}
\sin(\theta + \Delta\theta) - \sin\theta &= \sin\theta \cos\Delta\theta + \cos\theta \sin\Delta\theta - \sin\theta \\
&= \sin\Delta\theta \cos\theta + (\cos\Delta\theta - 1) \sin\theta \\
&= \beta\Delta\theta \cos\theta - \alpha\Delta\theta^2 \sin\theta.
\end{aligned}$$

Thus we have the basic difference formulae

$$\Delta \cos \theta = -\beta\Delta\theta \sin\theta - \alpha\Delta\theta^2 \cos\theta, \quad (10.2)$$

$$\Delta \sin \theta = \beta\Delta\theta \cos\theta - \alpha\Delta\theta^2 \sin\theta. \quad (10.3)$$

In contrast to continuous differentiation, we should note that the differences are *neither linear nor symmetric with respect to $\Delta\theta$* , due to the presence of $\Delta\theta^2$. This asymmetry will yield the discrepancy between the continuous and discrete cases in the following discussion. Moreover, differential algebraic relations such as $(\sin\theta)' = \cos\theta$ and $(\cos\theta)' = -\sin\theta$ do not hold in the discrete case, while the following phase shift relations are satisfied (Table 10.1):

$$\Delta \cos \theta = \cos(\theta + 2\Delta\theta),$$

$$\Delta \sin \theta = \sin(\theta + 2\Delta\theta).$$

10.3 Locomotion Under Nonholonomic Constraints

10.3.1 Derivation of the Continuous Single-Cart Model

Let us start with a simple example concerning planar locomotion of single rigid body, which we call a *single cart*, shown in Fig. 10.3(left). The state vector of this system is $\xi = (x_0, y_0, \theta_0) \in \mathcal{X}$, $\mathcal{X} := \mathbb{SE}(2)$ where (x_0, y_0) implies its position and θ_0 implies its orientation angle relative to the x -axis. We assume that the cart is not permitted to slide sideways. This means the *nonholonomic constraint*

$$\dot{y}_0 \cos\theta_0 - \dot{x}_0 \sin\theta_0 = 0 \quad (10.4)$$

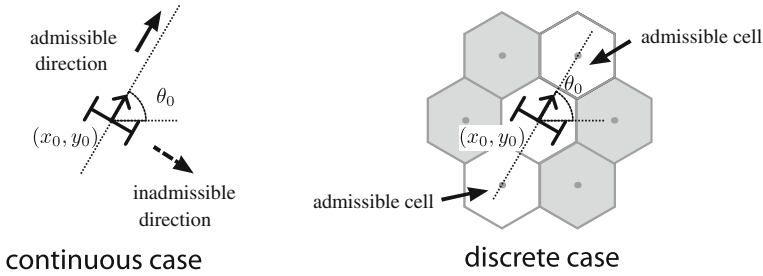


Fig. 10.3 Single cart: nonholonomic constraint imposed by the rolling wheels

should be satisfied. The state equation, derived from the kinematic relation, is given by the following differential equation

$$\dot{\xi} = g_1(\xi)u_1 + g_2(\xi)u_2, \quad (10.5)$$

$$g_1(\xi) := \begin{pmatrix} \cos \theta_0 \\ \sin \theta_0 \\ 0 \end{pmatrix}, \quad g_2(\xi) := \begin{pmatrix} 0 \\ 0 \\ 1 \end{pmatrix},$$

where $u_1 \in \mathbb{R}$ is the forwarding velocity and $u_2 \in \mathbb{R}$ is the heading angular velocity. Each point $\xi \in \mathcal{X}$ can be an equilibrium by setting $u = 0$. Brockett's stabilizability theorem [2] tells us that this system is *not asymptotically stabilizable* by any smooth time-invariant state feedback law. This system, in turn, is called *controllable* if any two equilibria can be reached from each other [10]. This is indeed satisfied since its controllability Lie algebra

$$\mathcal{C}(\xi) := \text{span}\{g_1(\xi), g_2(\xi), [g_1, g_2](\xi)\} \quad (10.6)$$

has dimension 3 at $\forall \xi \in \mathcal{X}$, where

$$[g_1, g_2](\xi) := \frac{\partial g_2}{\partial \xi} g_1 - \frac{\partial g_1}{\partial \xi} g_2 = \begin{pmatrix} \sin \theta_0 \\ -\cos \theta_0 \\ 0 \end{pmatrix}.$$

10.3.2 Derivation of the Discrete Version

Now let us discuss what happens if the single cart is placed on the hexagonal cellular space (Fig. 10.3, right). The state vector of this system is $\xi = (x_0, y_0, \theta_0)$ as the same as in the continuous case, but it must be an element of $\mathcal{X} = \mathbb{SE}_H(2)$.

Next, let us think of a condition which prevents the cart from sliding sideways. Let Δx_0 denote the progress of the variable x_0 from the current step k to the next step $k + 1$, i.e.,

$$\Delta x_0 = x_0[k + 1] - x_0[k]. \tag{10.7}$$

Δy_0 and $\Delta \theta_0$ are defined in the same manner. Then the discrete version of the nonholonomic constraint is given by

$$\Delta y_0 \cos \theta_0 - \Delta x_0 \sin \theta_0 = 0. \tag{10.8}$$

Suppose $u_1 \in \{-1, 0, 1\}$ is the forwarding velocity and $u_2 \in \{-1, 0, 1\}$ is the heading angular velocity. Then the state equation of the cart is immediately obtained as

$$\begin{pmatrix} \Delta x_0 \\ \Delta y_0 \\ \Delta \theta_0 \end{pmatrix} = \begin{pmatrix} \cos \theta_0 \\ \sin \theta_0 \\ 0 \end{pmatrix} u_1 + \begin{pmatrix} 0 \\ 0 \\ 1 \end{pmatrix} u_2, \tag{10.9}$$

or equivalently,

$$\Delta \xi = g_1(\xi)u_1 + g_2(\xi)u_2, \tag{10.10}$$

$$g_1(\xi) := \begin{pmatrix} \cos \theta_0 \\ \sin \theta_0 \\ 0 \end{pmatrix}, \quad g_2(\xi) := \begin{pmatrix} 0 \\ 0 \\ 1 \end{pmatrix}.$$

The process of this derivation is summarized in Fig. 10.4. What we have derived here is an integer-valued difference equation *that satisfies the discrete nonholonomic constraint (10.8)*, which should be distinguished from a direct discretization of the continuous differential equation (10.5) although it apparently seems to be.

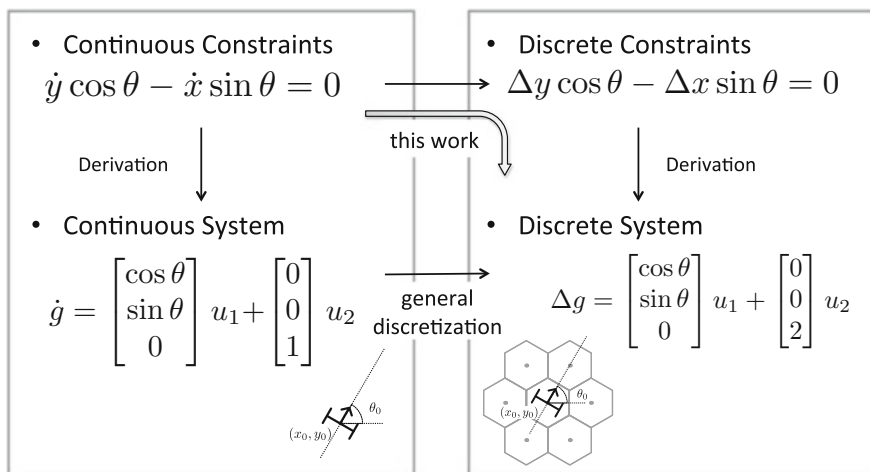


Fig. 10.4 Overview of the discretization approach in this work. At first, the continuous constraint (nonholonomic velocity constraint) is replaced by its discrete counterpart, then the description of dynamics (state equation) is derived which conform to the constraint

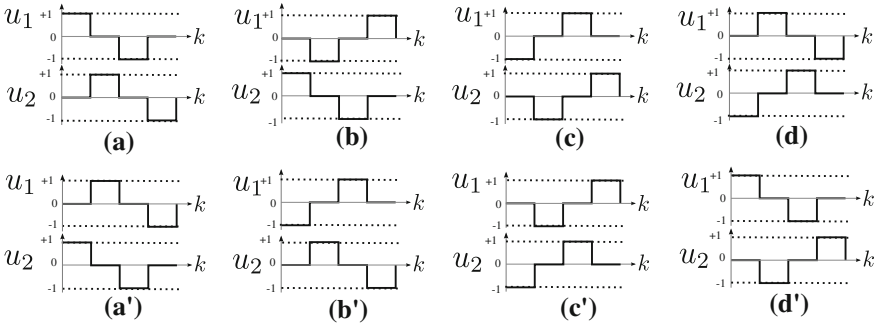


Fig. 10.5 Primitive periodic input patterns. Sequence of control inputs $u_1[k], u_2[k] \in \{1, 0, -1\}$ are chosen so that each of their average over a period is zero

10.3.3 Holonomy and the Lie Bracket Motion

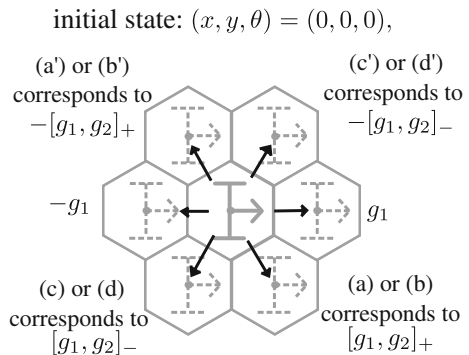
Using the discrete model of a single cart obtained above, let us investigate discrete version of *holonomy*, i.e., the net effect of periodic inputs. Figure 10.5 shows primitive 8 patterns of four step periodic input signals with unit amplitude. The input (a') is the time-reversal signal of (a) and vice versa, and so for other pairs.

Figure 10.6 shows the effect of these inputs starting from the origin. The effect of (a') is just the opposite to that of (a) and so for the other pairs. In essence, the holonomy is split into two types, the effect of (a)(b) and that of (c)(d).

As an analogy from the continuous case, we expect it possible to analyze this effect by some discrete counterpart of Lie bracket. For this purpose, let us first define discrete version of Jacobian matrix.

$$\Delta g_1 = g_1(\xi + \Delta\xi) - g_1(\xi) = \begin{pmatrix} -\beta\Delta\theta_0 S_0 - \alpha\Delta\theta_0^2 C_0 \\ \beta\Delta\theta_0 C_0 - \alpha\Delta\theta_0^2 S_0 \\ 0 \end{pmatrix},$$

Fig. 10.6 Effect of Lie bracket; motions of the single cart resulting from the periodic input patterns



where $S_0 = \sin \theta_0$, $C_0 = \cos \theta_0$. The problem here is that Δg_1 is not linear with respect to $\Delta \xi$ due to the presence of $\Delta \theta_0^2$. Now, let us remember that $\Delta \theta_0^2$ may be replaced by the linear term, i.e., $\Delta \theta_0^2 = \Delta \theta_0$ if $\Delta \theta_0 \geq 1$, while $\Delta \theta_0^2 = -\Delta \theta_0$ if $\Delta \theta_0 \leq -1$. Then this leads us to define *two branches* of Jacobians $J_+(g_1)$ and $J_-(g_1)$, as follows:

$$J_+(g_1) := \begin{pmatrix} 0 & 0 & -\beta S_0 - \alpha C_0 \\ 0 & 0 & \beta C_0 - \alpha S_0 \\ 0 & 0 & 0 \end{pmatrix}, \quad J_-(g_1) := \begin{pmatrix} 0 & 0 & -\beta S_0 + \alpha C_0 \\ 0 & 0 & \beta C_0 + \alpha S_0 \\ 0 & 0 & 0 \end{pmatrix},$$

which enable us to rewrite Δg_1 as

$$\Delta g_1 = \begin{cases} J_+(g_1)\Delta \xi, & \text{if } \Delta \theta_0 \geq 0, \\ J_-(g_1)\Delta \xi, & \text{if } \Delta \theta_0 \leq 0. \end{cases}$$

Using J_+ and J_- , we can define the following two branches of Lie brackets:

$$[g_1, g_2]_+(\xi) := J_+(g_2)g_1 - J_+(g_1)g_2 = \begin{pmatrix} \beta S_0 + \alpha C_0 \\ -\beta C_0 + \alpha S_0 \\ 0 \end{pmatrix},$$

$$[g_1, g_2]_-(\xi) := J_-(g_2)g_1 - J_-(g_1)g_2 = \begin{pmatrix} \beta S_0 - \alpha C_0 \\ -\beta C_0 - \alpha S_0 \\ 0 \end{pmatrix}.$$

Their values at $\xi = 0$ are:

$$g_1(0) = \begin{pmatrix} 1 \\ 0 \\ 0 \end{pmatrix}, \quad g_2(0) = \begin{pmatrix} 0 \\ 0 \\ 1 \end{pmatrix}, \quad [g_1, g_2]_+(0) = \begin{pmatrix} \alpha \\ -\beta \\ 0 \end{pmatrix}, \quad [g_1, g_2]_-(0) = \begin{pmatrix} -\alpha \\ -\beta \\ 0 \end{pmatrix},$$

which are consistent with the actual displacements shown in Fig. 10.6.

10.4 Connected Rigid Bodies: Locomotion Under both Nonholonomic and Holonomic Constraints

10.4.1 Cart-Trailer Systems

In this section, we consider planar locomotion of multiple rigid bodies connected to each other. Suppose a cart towing ℓ trailers as shown in Fig. 10.7(left). Each of the carts $0, \dots, \ell - 1$ has a free joint on the center of its wheel axis, which connects the following cart to itself. The length of each connecting link is supposed to be 1. The state vector is

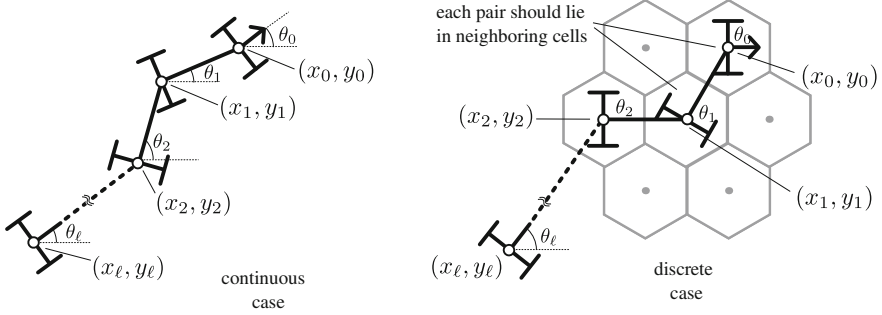


Fig. 10.7 Cart-trailer system is composed of a heading cart with articulated trailers, which undergoes holonomic constraints due to rigid linkage

$$\begin{aligned}\xi &= (x_0, y_0, \theta_0, \dots, \theta_\ell)^\top \in \mathcal{X}, \\ \mathcal{X} &:= \mathbb{SE}(2) \times \mathbb{T}^{\ell-1},\end{aligned}$$

where (x_0, y_0) denotes the position of the truck (cart 0) and θ_i denotes the orientation of the cart i for $i = 0, \dots, \ell$. This system undergoes $\ell + 1$ nonholonomic constraints

$$\dot{y}_i \cos \theta_i - \dot{x}_i \sin \theta_i = 0, \quad i = 0, \dots, \ell - 1 \quad (10.11)$$

and ℓ *holonomic constraints* of rigid linkage as well:

$$\begin{cases} x_i = x_{i+1} + \cos \theta_{i+1}, & i = 0, \dots, \ell - 1. \\ y_i = y_{i+1} + \sin \theta_{i+1}, \end{cases}$$

We also have to pay attention to the joint limitation

$$|\theta_{i+1} - \theta_i| < \pi, \quad i = 0, \dots, \ell - 1.$$

By taking all the constraints into account, the state equation is obtained as

$$\dot{\xi} = g_1(\xi)u_1 + g_2(\xi)u_2, \quad (10.12)$$

$$g_1(\xi) := \begin{pmatrix} \cos \theta_0 \\ \sin \theta_0 \\ 0 \\ -\sin(\theta_1 - \theta_0) \\ -\sin(\theta_2 - \theta_1) \cos(\theta_1 - \theta_0) \\ \vdots \end{pmatrix}, \quad g_2(\xi) := \begin{pmatrix} 0 \\ 0 \\ 1 \\ 0 \\ 0 \\ \vdots \end{pmatrix},$$

where u_1 is the forwarding velocity and u_2 is the heading angular velocity of the truck (cart 0). It is easy to show that this system is also controllable by analyzing its controllability Lie algebra.

10.4.2 Derivation of the Discrete Version

Now let us turn to consider the discrete counterpart (Fig. 10.7, right). Each cart is placed on the hexagonal cells, thus each joint angle is the difference between adjoining cart orientation, e.g., $\theta_{i+1} - \theta_i$. We also assume that the joint angles are limited to

$$|\theta_{i+1} - \theta_i| < 3, \quad i = 0, \dots, \ell - 1.$$

The state vector is

$$\begin{aligned} \xi &= (x_0, y_0, \theta_0, \dots, \theta_\ell)^\top \in \mathcal{X}, \\ \mathcal{X} &:= \text{SE}_H(2) \times \mathbb{Z}_6^{\ell-1}. \end{aligned}$$

Control inputs are assigned to the velocity of the trucks, i.e., u_1 is the forwarding velocity and u_2 is the heading angular velocity of the front cart, respectively:

$$\begin{aligned} \Delta x_0 C_0 + \Delta y_0 S_0 &= u_1, \\ \Delta \theta_0 &= u_2 \text{ of}. \end{aligned} \tag{10.13}$$

Nonholonomic constraint for the wheels are

$$\Delta y_i C_i - \Delta x_i S_i = 0, \quad i = 0, \dots, \ell. \tag{10.14}$$

Holonomic constraints for rigid linkage are

$$\begin{cases} x_{i-1} = x_i + C_i, \\ y_{i-1} = y_i + S_i, \end{cases} \quad i = 1, \dots, \ell. \tag{10.15}$$

The holonomic constraints should be kept satisfied in every step; hence the constraints in the next step

$$\begin{cases} (x_{i-1} + \Delta x_{i-1}) = (x_i + \Delta x_i) + \cos(\theta_i + \Delta \theta_i), \\ (y_{i-1} + \Delta y_{i-1}) = (y_i + \Delta y_i) + \sin(\theta_i + \Delta \theta_i) \end{cases} \tag{10.16}$$

should also hold for $i = 1, \dots, \ell$. The state vector of this system is

$$\xi = (x_0, y_0, \theta_0, \dots, \theta_\ell) \in \mathbb{S}\mathbb{E}_H(2) \times \mathbb{Z}_6^{\ell-1}.$$

In order to obtain a difference equation for this system, we have to eliminate $\Delta x_1, \dots, \Delta x_\ell, \Delta y_1, \dots, \Delta y_\ell, x_1, \dots, x_\ell, y_1, \dots, y_\ell$ from (10.13)–(10.16) and derive explicit expression of $\Delta \xi$. (We eliminate 4ℓ variables from $5\ell + 3$ equations, resulting in $\ell + 3$ solutions). First, substituting (10.2), (10.3) and (10.15) into (10.16), we have

$$\begin{cases} \Delta x_{i-1} = \Delta x_i - \beta \Delta \theta_i S_i - \alpha \Delta \theta_i^2 C_i, \\ \Delta y_{i-1} = \Delta y_i + \beta \Delta \theta_i C_i - \alpha \Delta \theta_i^2 S_i, \end{cases}$$

or equivalently,

$$\begin{cases} \Delta x_i = \Delta x_0 + \sum_{j=1}^i (\beta \Delta \theta_j S_j + \alpha \Delta \theta_j^2 C_j), \\ \Delta y_i = \Delta y_0 + \sum_{j=1}^i (-\beta \Delta \theta_j C_j + \alpha \Delta \theta_j^2 S_j). \end{cases}$$

Computing $\Delta y_{i-1} C_i - \Delta x_{i-1} S_i$ leads us

$$\Delta y_{i-1} C_i - \Delta x_{i-1} S_i = \Delta y_i C_i - \Delta x_i S_i + \beta \Delta \theta_i = \beta \Delta \theta_i,$$

where the nonholonomic constraints (10.14) are used. Thus $\Delta \theta_i$ can be obtained by recursive computation

$$\begin{aligned} \beta \Delta \theta_i &= \Delta y_{i-1} C_i - \Delta x_{i-1} S_i \\ &= \Delta y_0 C_i - \Delta x_0 S_i - \sum_{j=1}^{i-1} \left(\beta \Delta \theta_j (C_i C_j + S_i S_j) + \alpha \Delta \theta_j^2 (S_i C_j - C_i S_j) \right) \\ &= -S_{i0} u_1 - \sum_{j=1}^{i-1} \left(\beta \Delta \theta_j C_{ij} - \alpha \Delta \theta_j^2 S_{ij} \right), \end{aligned} \tag{10.17}$$

where $C_{ij} = \cos(\theta_i - \theta_j)$, $S_{ij} = \sin(\theta_i - \theta_j)$.

10.4.2.1 Single Trailer

The simplest case is a single trailer system ($\ell = 1$), whose state vector is $\xi = (x_0, y_0, \theta_0, \theta_1)^\top$. The state equation is given by

$$\Delta \xi = g_1(\xi) u_1 + g_2(\xi) u_2,$$

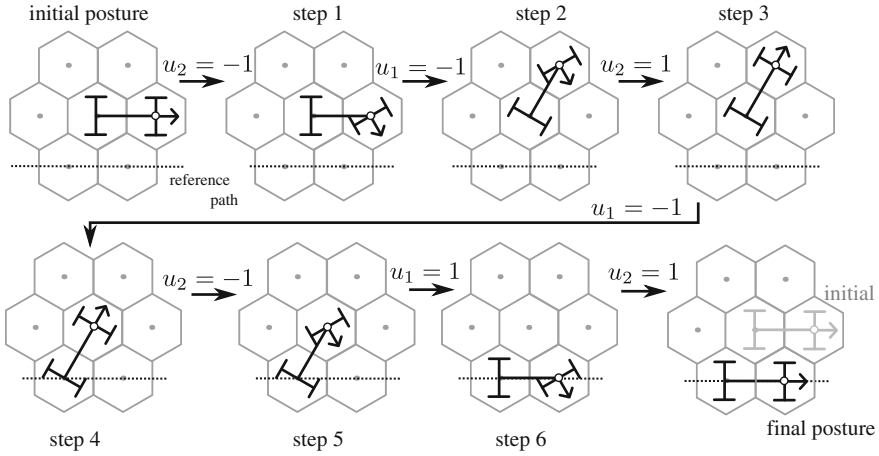


Fig. 10.8 Backward parking of the single trailer for linear reference path. The vehicle moves rightward in parallel from the initial position

$$g_1(\xi) = \begin{pmatrix} C_0 \\ S_0 \\ 0 \\ -S_{10}/\beta \end{pmatrix}, \quad g_2(\xi) = \begin{pmatrix} 0 \\ 0 \\ 1 \\ 0 \end{pmatrix}. \tag{10.18}$$

Forwarding motion this trailer system is not difficult to imagine from the single cart case. Backward motion is also possible, e.g., by a skillful steering shown in Fig. 10.8.

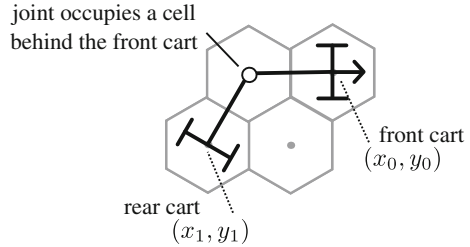
10.4.2.2 Double Trailers

When the cart is towing two trailers, i.e., if $\ell = 2$, the state vector is $\xi = (x_0, y_0, \theta_0, \theta_1, \theta_2)$. Behavior of the first four state variables is as exactly the same as in the previous case (10.18), while $\Delta\theta_2$ can be derived using (10.17) as follows:

$$\begin{aligned} \beta \Delta\theta_2 &= -S_{20}u_1 - \beta \Delta\theta_1 C_{21} - \alpha \Delta\theta_1^2 S_{21} \\ &= -S_{20}u_1 + \beta S_{21} C_{10} u_1 \beta - \frac{\alpha}{\beta^2} S_{21} S_{10}^2 u_1^2 \\ &= -S_{21} C_{10} u_1 - \frac{\alpha}{\beta^2} S_{21} S_{10}^2 u_1^2. \end{aligned}$$

Note that the state equation is not linear with respect to u_1 any longer; this implies the system behavior changes depending on the sign of u_1 .

Fig. 10.9 Trailer with off-axle hitching; the joint is located in the middle of two carts



10.4.2.3 Trailer with Off-Axle Hitching

Suppose that the hinge joint is not precisely at the center of the rear axis (see Fig. 10.9). This configuration is so-called *off-axle hitching*, where its behavior is slightly different from the previous case. In this case, the holonomic constraint (10.15) is replaced by

$$\begin{cases} x_{i-1} = x_i + C_i + C_{i-1}, \\ y_{i-1} = y_i + S_i + S_{i-1}, \end{cases} \quad i = 1, \dots, \ell. \quad (10.19)$$

The state equation is obtained by solving (10.19) and (10.14) for $(\Delta x_0, \Delta y_0, \Delta \theta_0, \dots, \Delta \theta_\ell)$. The single trailer case ($\ell = 1$) is given as follows:

$$\Delta \xi = \begin{pmatrix} C_0 \\ S_0 \\ 0 \\ -S_{10}/\beta \end{pmatrix} u_1 + \begin{pmatrix} 0 \\ 0 \\ u_2 \\ -C_{10}u_2 - \alpha S_{10}u_2^2/\beta \end{pmatrix}. \quad (10.20)$$

Unlike the on-axle case, the right-hand side is not linear in u_2 any longer, and the steering input u_2 affects both $\Delta \theta_0$ and $\Delta \theta_1$.

10.5 Reachability Issues

Now we proceed to discuss a crucial problem to observe the region that the mobile robots can reach from given initial state. In the case of continuous systems, we could apply continuous-valued inputs to mobile robots. In the discrete-valued cases, however, we can give only discrete-valued inputs and robots placed on the hexagonal cellular space. This causes essential differences of reachable state between continuous systems and discrete-valued nonholonomic mobile robot systems. In this section, we define a *stepwise reachability set* as the collection of all reachable states within the given number of steps.

10.5.1 Definitions

We restart with a slightly general formulation of system dynamics, where the state equation of a discrete-valued nonholonomic mobile robot systems is expressed as the following difference equation of integral values:

$$\xi[k + 1] = \xi[k] + \Delta\xi = \mathbf{G}(\xi[k], u[k]). \quad (10.21)$$

Let $\{u[k]|k \in \mathbb{Z}_+\}$ be a series of inputs to be applied. Then the stepwise evolution of the system state is given by

$$\begin{aligned} \xi[1] &= \mathbf{G}(\xi[0], u[0]) &&= \mathbf{G}_1(\xi[0], u[0]), \\ \xi[2] &= \mathbf{G}(\xi[1], u[1]) &&= \mathbf{G}_2(\xi[0], u[0], u[1]), \\ &\vdots &&\vdots \\ \xi[k] &= \mathbf{G}(\xi[k-1], u[k-1]) &&= \mathbf{G}_k(\xi[0], u[0], \dots, u[k-1]), \end{aligned}$$

where \mathbf{G}_k is recursively defined by

$$\begin{aligned} \mathbf{G}_{k+1}(\xi[0], u[0], \dots, u[k-1]) &:= \mathbf{G}(\mathbf{G}_{k-1}(\xi[0], u[0], \dots, u[k-2]), u[k-1]), \\ \mathbf{G}_1(\xi[0], u[0]) &:= \mathbf{G}(\xi[0], u[0]). \end{aligned}$$

Definition 10.1 (*Stepwise Reachability Set*) For the integer-valued difference equations (10.21), the k -stepwise reachability set from the state $\xi[0]$, denoted by $\Lambda(\xi[0], k)$, is defined as

$$\Lambda(\xi[0], k) := \{\mathbf{G}_k(\xi[0], u[0], \dots, u[k-1]), u[j] \in \Omega, j = 0, \dots, k-1\},$$

where Ω is the set of all admissible inputs.

Definition 10.2 (*Neighborhood*) For an integer-valued state $\xi \in \mathbb{Z}^N$, its neighborhood is defined as

$$N(\xi) := \{\xi + (\delta_1, \dots, \delta_N)^\top, \delta_i \in \{-1, 0, 1\}, i = 1, \dots, N\}.$$

10.5.2 Application

Let us turn to consider how the k -stepwise reachability set grows as k increases, when applied to the case of wheeled mobile robot we discussed in Sect. 10.3. Figure 10.10 shows a visualization of the k -stepwise reachability set of the single cart from $\xi[0] = (0, 0, 0)^\top$.

In Fig. 10.10, thick-lined hexagons imply the reachable cells by k steps for $k = 1, 2, 3, 4$. These cells contain some colored triangles, which imply the reachable ‘‘orientation’’ by k steps. For instance, the 1-step reachability set consists of

$$(0, 0, 0)^T, (0, 0, 1)^T, (0, 0, -1)^T, (1, 0, 0)^T, (-1, 0, 0)^T.$$

At $k = 1$, the cart can move only in the initial orientation due to the nonholonomic constraint (10.8), namely, it cannot step sideways. Next, in the 2-stepwise reachability set, the cart can move to cells around the initial cell. However, the orientation of the cart is different from the initial orientation. Therefore, the cart can not take any state. Finally, the 4-stepwise reachability set shows that the cart can move to all the neighboring cells around the initial one with arbitrary orientations there. This analysis results in the fact

$$\arg \min_k \{ \Lambda(\xi[0, k]) \supseteq N(\xi[0]) \} = 4.$$

This indicates us a sufficient condition for controllability. By repeating these primitive motions to neighboring cells, each of which is composed of 4 steps at most, the state of the single cart can be transferred to *any* desired state in the whole hexagonal space. In addition, the 4-step reachability set in Fig. 10.10 indicates the same property as the continuous case that it is easy for the cart to move in the same direction as the initial orientation.

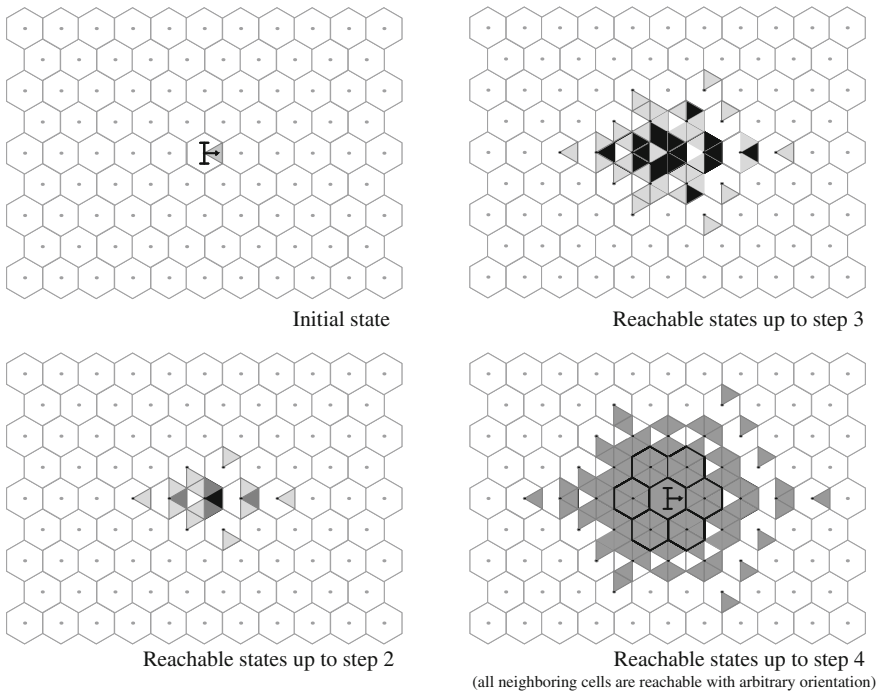


Fig. 10.10 Stepwise reachability set planar locomotion under discrete nonholonomic constraint. the *grey triangles* indicate the reachable states (considering its position and orientation) within the specified steps. All the neighboring cells are reachable up to 4 steps with arbitrary orientation

10.6 Other Possibilities of Cellular Tesselation

Thus far, we adopt regular hexagons for spatial discretization, mainly focusing on its preferable properties such as isotropy, e.g., distance between neighboring centers is always 1. Of course, this is not the only choice. The \mathbb{R}^2 can also be filled with regular squares or regular triangles as shown in Fig. 10.11. In this final section, let us pursue the possibility of square tesselation.

Positions of the cells can be addressed by the usual Cartesian coordinate system (Fig. 10.11). Here we have two choices in defining adjacency; one is the so-called *Neumann neighborhood*, where each square cell is adjacent to 4 cells via its edges (i.e., its top, bottom, right and left sides). Then the discrete space is associated with 4 directions, namely,

$$\mathbb{S}\mathbb{E}_N(2) = \left\{ \begin{pmatrix} x \\ y \\ \theta \end{pmatrix} = \begin{pmatrix} n_x \alpha \\ n_y \beta \\ n_\theta \gamma \end{pmatrix} \middle| n_x, n_y \in \mathbb{Z}, n_\theta \in \mathbb{Z}_4 \right\} \simeq \mathbb{Z} \times \mathbb{Z} \times \mathbb{Z}_4,$$

where $\mathbb{Z}_4 = \{0, 1, 2, 3\} \equiv \{0, \pm 1, 2\}$ and $\alpha = 1, \beta = 1, \gamma = \frac{\pi}{2}$. The other is the so-called *Moore neighborhood*, where each square cell is adjacent to 8 cells via its vertices as well as edges (i.e., all the surrounding cells). Then the discrete space is associated with 8 directions, namely,

$$\mathbb{S}\mathbb{E}_M(2) = \left\{ \begin{pmatrix} x \\ y \\ \theta \end{pmatrix} = \begin{pmatrix} n_x \alpha \\ n_y \beta \\ n_\theta \gamma \end{pmatrix} \middle| n_x, n_y \in \mathbb{Z}, n_\theta \in \mathbb{Z}_8 \right\} \simeq \mathbb{Z} \times \mathbb{Z} \times \mathbb{Z}_8,$$

where $\mathbb{Z}_8 = \{0, 1, 2, 3, 4, 5, 6, 7\} \equiv \{0, \pm 1, \pm 2, \pm 3, 4\}$ and $\alpha = 1, \beta = 1, \gamma = \frac{\pi}{4}$.

The cosine and sine function and its derivatives can be defined as before, shown in Fig. 10.12 and Tables 10.2 and 10.3. Note that all the values concerned here are limited to +1, 0, -1.

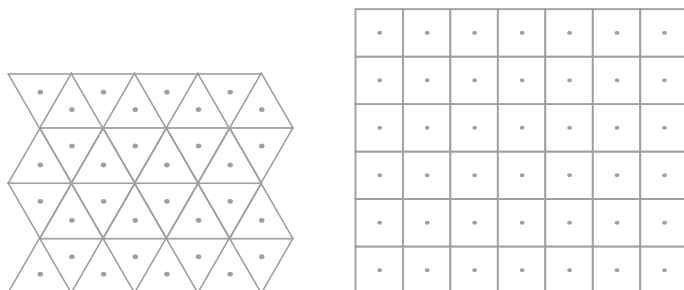


Fig. 10.11 Alternate choices of regular tessellations for \mathbb{R}^2 (left triangular, right square)

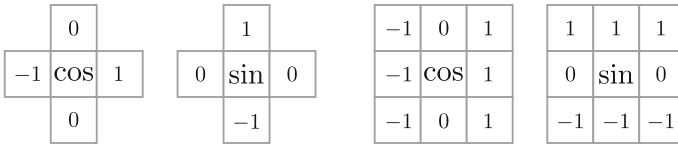


Fig. 10.12 Cosine and sine on square cells (*left* Neumann, *right* Moore)

Table 10.2 Discrete trigonometric calculus on square cells (Neumann neighborhood)

$\Delta \cos \theta$				
	$\theta = -1$	$\theta = 0$	$\theta = 1$	$\theta = 2$
$\Delta\theta = 1$	1	-1	-1	1
$\Delta\theta = -1$	-1	-1	1	1
$\Delta \sin \theta$				
$\Delta\theta = 1$	1	1	-1	-1
$\Delta\theta = -1$	1	-1	-1	1

Table 10.3 Discrete trigonometric calculus on square cells (Moore neighborhood)

$\Delta \cos \theta$								
	$\theta = -3$	$\theta = -2$	$\theta = -1$	$\theta = 0$	$\theta = 1$	$\theta = 2$	$\theta = 3$	$\theta = 4$
$\Delta\theta = 1$	1	1	0	0	-1	-1	0	0
$\Delta\theta = -1$	0	-1	-1	0	0	1	1	0
$\Delta \sin \theta$								
$\Delta\theta = 1$	0	0	1	1	0	0	-1	-1
$\Delta\theta = -1$	1	0	0	-1	-1	0	0	1

Now the discrete version of nonholonomic wheel constraint for a single cart is expressed as

$$\Delta y_0 \cos \theta_0 - \Delta x_0 \sin \theta_0 = 0$$

for both cases of the Neumann and Moore neighborhood. This leads us to derive the corresponding cart kinematics

$$\Delta \xi = g_1(\xi)u_1 + g_2(\xi)u_2, \tag{10.22}$$

$$g_1(\xi) := \begin{pmatrix} \cos \theta_0 \\ \sin \theta_0 \\ 0 \end{pmatrix}, \quad g_2(\xi) := \begin{pmatrix} 0 \\ 0 \\ 1 \end{pmatrix},$$

which is apparently the same as the hexagonal version (10.10). Notable difference can be found in the corresponding Lie-bracket motions, as shown in Fig. 10.13

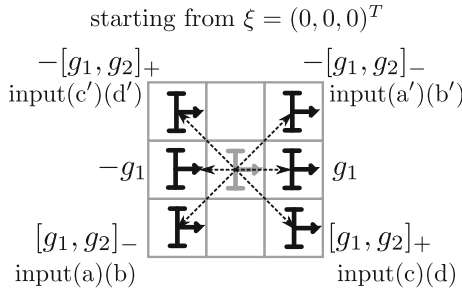


Fig. 10.13 Lie bracket motions of the single cart on square cells (Neumann neighborhood)

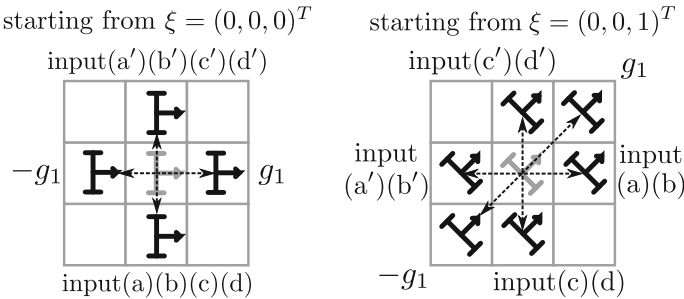


Fig. 10.14 Lie bracket motions of the single cart on square cells (Moore neighborhood)

and Fig. 10.14. In particular, for the case of Moore neighborhood, the net effects are different between $\theta = 0, 2, 4, 6$ and $\theta = 1, 3, 5, 7$, depending on multi-valuedness of the corresponding Lie bracket operations (see Fig. 10.6 for comparison).

10.7 Conclusion

In this chapter, we discussed possibility of discrete-valued version of locomotion of rigid bodies on the horizontal plane. We showed that, many *intrinsic properties consistent with the continuous case* can be derived starting from simply defined discrete constraints. We also examined the k -stepwise reachability set $\Lambda(\xi[0], k)$ for these systems, to confirm possibility to maneuver the system state to any states. Other cases including both holonomic and nonholonomic constraints, and alternate possibilities on cellular tessellation were also discussed.

We showed only a clue to respond to the authors' primitive motivations in this chapter. It is not surprising that a lot of unsolved problems to be discussed are left for the future works; For example, stability and stabilization issues are not discussed at all. Characterization of stability must be crucial in developing theoretical analysis of system behavior. The typical Lyapunov approach may have a difficulty, in the sense

that the converse theorem is not likely to hold in discrete-valued (i.e., discontinuous) cases. Moreover, discrete version of Brockett's theorem [2] must be a quite interesting issue. Other topics contain control *design* theory, e.g., design of discontinuous, time-varying or hybrid controllers have been central issues of continuous nonholonomic systems. Some ideas of existing design approaches, e.g., time-varying approaches [8], may remain effective in discrete cases.

The authors believe it important to discuss if there exists any *underlying mechanics/physics as first principle*, i.e., discrete equivalents of energy, Lagrangian, Hamiltonian or variational principle that are consistent with the current results. It would also be interesting to relate it with discrete mechanics proposed by Marsden et al. [5]. The current work can be considered a *Lebesgue*-type approach to discrete mechanics, in contrast that the aforementioned one [5] can be regarded as a *Riemann*-type approach.

The authors expect the current work to be a first step toward establishment of discrete-valued nonlinear system theory under spatial symmetry.

Acknowledgments The authors are grateful to continuous encouragement by Professor Koichi Osuka.

References

1. Barraquand, J., Latombe, J.C.: Nonholonomic multibody mobile robots: controllability and motion planning in the presence of obstacles. *Algorithmica* **10**, 121–155 (1993)
2. Brockett, R.W.: Asymptotic stability and feedback stabilization. In: Brockett, R.W., Millman, R.S., Sussman, H. (eds.) *Differential Geometric Control Theory*, pp. 181–191. Birkhauser, Boston (1983)
3. Hirota, R., Takahashi, D.: *Discrete and Ultradiscrete Systems*. Kyoritsu Publishing, Tokyo (2003) (in Japanese)
4. Kita, T., Ishikawa, M., Osuka, K.: On discrete-valued modeling of nonholonomic mobile robot systems. In: 2012 IEEE International Conference on Robotics and Biomimetics (ROBIO2012), pp. 2024–2031 (2012)
5. Marsden, J.E., West, M.: Discrete mechanics and variational integrators. *Acta Numerica* **10**, 357–514 (2001)
6. Middleton, L., Sivaswamy, J.: *Hexagonal Image Processing*. Advances in Computer Vision and Pattern Recognition. Springer, New York (2005)
7. Monaco, S., Noman-Cyrot, D.: A unified representation for nonlinear discrete-time and sampled dynamics. *J. Math. Syst. Estim. Control* **7**(4), 477–503 (1997)
8. Morin, P., Samson, C.: Practical stabilization of driftless systems on lie groups: the transverse function approach. *IEEE Trans. Autom. Control* **48**(9), 1496–1508 (2003)
9. Netic, D., Teel, A.: A framework for stabilization of nonlinear sampled-data systems based on their approximate discrete-time models. *IEEE Trans. Autom. Control* **49**(7), 1103–1122 (2004)
10. Nijmeijer, H., van der Schaft, A.J.: *Nonlinear Dynamical Control Systems*. Springer, New York (1990)
11. Schiff, J.: *Cellular Automata: A Discrete View of the World*. Wiley, Hoboken (2008)
12. Wolfram, S.: *Cellular Automata and Complexity: Collected Papers*. Westview, Boulder (1994)
13. Yuz, J.I., Goodwin, G.C.: On sampled-data models for nonlinear systems. *IEEE Trans. Autom. Control* **50**(10), 1477–1489 (2005)